Journal of ELECTRONIC MATERIALS, Vol. 38, No. 1, 2009
DOI: 10.1007/s11664-008-0577-2
© 2008 TMS
Regular Issue Paper

Optical Characteristics of ZnTeO Thin Films Synthesized by Pulsed Laser Deposition and Molecular Beam Epitaxy

W. WANG,[1,2] W. BOWEN,[1] S. SPANNINGA,[1] S. LIN,[1] and J. PHILLIPS[1]

1.—Department of Electrical Engineering and Computer Science, The University of Michigan, Ann Arbor, MI 48109-2122, USA. 2.—e-mail: umwwm@umich.edu

Oxygen incorporation into ZnTe was studied using pulsed laser deposition and molecular beam epitaxy. Oxygen incorporation at the high partial pressures studied for pulsed laser deposition was found to result in increasing visible transparency with oxygen incorporation, and is attributed to the formation of TeO_x based on bonding information obtained by x-ray photoelectron spectroscopy measurements. Oxygen incorporation by a plasma source during the growth of ZnTe by molecular beam epitaxy was found to result in an electronic band at 0.5 eV below the ZnTe band edge, possessing strong radiative properties and a resonant-like optical absorption coefficient with a peak $\alpha > 5000\ cm^{-1}$. The ZnTeO thin films grown by MBE have an epitaxial structure similar to ZnTe, where it is unclear whether the properties are due to the formation of a high-density defect level or the formation of a dilute alloy.

Key words: ZnTeO, diluted alloy, defect level, absorption coefficient

INTRODUCTION

Wide-bandgap semiconductors based on ZnO, ZnTe, and related II–VI compound semiconductors are attractive for several device applications including light emitters and detectors operating in the visible/ultraviolet spectral region, and transparent electronics. Research and development efforts on alloys related to ZnO have predominantly focused on the mixed cation materials CdZnO, MgZnO, and BeZnO. Mixed anion alloys related to ZnO such as ZnO(S,Se,Te) may also provide the ability to tune the semiconductor bandgap energy in the visible and ultraviolet spectral region, but are less well understood. ZnTe has a direct bandgap at 2.29 eV, corresponding to the green optical wavelength, and has been investigated in great detail for application to ZnSe-based visible light emitters, CdZnTe x-ray detectors, and ZnTe buffer layers for HgCdTe infrared detectors. ZnTe has shown the ability for controllable *p*-type doping by nitrogen,[1–4] with hole concentrations of up to $10^{20}\ cm^{-3}$. The source of the unique *p*-type nature for this wide-bandgap material is believed to be the native defect structure, where defects lie within the valence band rather than within the bandgap.[5] The unique *p*-type behavior of ZnTe, a notorious problem for ZnO and many wide-bandgap semiconductors, and the possibility for a tunable bandgap energy in the visible spectral region make alloys of ZnTeO potentially attractive materials for optoelectronic devices.

Compared with oxygen doping in CdTe, where oxygen acts as a shallow acceptor,[6] doping or alloying of ZnTe with oxygen is believed to result in a highly mismatched alloy, in which Te and O atoms possess a very different electronegativity. In the extreme of low oxygen concentration, a substitutional impurity of O_{Te} in ZnTe results in a defect level 0.4 eV from the conduction band and a strong radiative transition at 1.9 eV.[7,8] This strong radiative transition in ZnTe:O has in fact been used in red light emission diodes,[9] and also a phosphorescent material for x-ray detectors, where long radiative lifetimes of $>1\ \mu s$ have been reported.[10] A higher oxygen content in ZnTe is predicted to introduce a narrow electronic band in the material, as explained by a band anticrossing model.[11]

(Received May 29, 2008; accepted September 23, 2008; published online October 21, 2008)

Experiments and calculations have suggested the presence of such an intermediate band in ZnTeO and the quaternary ZnMnTeO.[11] Bandgap reduction in ZnTe with the introduction of oxygen has also been reported by other research groups recently,[12,13] providing further evidence of an intermediate band in this alloy. In this work, the synthesis of ZnTeO thin films by pulsed laser deposition and molecular beam epitaxy is investigated to further examine the possible formation of an intermediate band or alloy system spanning the visible/ultraviolet (UV) spectral region.

EXPERIMENT

ZnTeO thin films are synthesized using both pulsed laser deposition and molecular beam epitaxy. Pulsed laser deposition (PLD) was used to study the ZnTeO thin-film deposition under a relatively high oxygen partial pressure. Samples were deposited on both c-plane sapphire and GaAs (001) substrates using a ZnTe target, KrF excimer laser (λ = 248 nm, 20 ns pulse width, 6 Hz repetition rate), a deposition temperature of 300°C, and varying ambients of high vacuum ($<5 \times 10^{-6}$ Torr), nitrogen, or oxygen. Deposition by PLD under nitrogen or oxygen conditions was done with a partial pressure in the range of 10 mTorr to 100 mTorr. Nitrogen incorporation is studied in this work as a form of experimental control, allowing separate comparison of differing chemical species and differing deposition partial pressure. The growth rate under these conditions was varied from approximately 0.4 nm/s to 1.1 nm/s, with a sample thickness in the range of 0.7 μm to 1.9 μm. Molecular beam epitaxy (MBE) was used to study ZnTeO growth under low oxygen partial pressure. MBE growth was performed with a base pressure near 10^{-9} Torr at a substrate temperature of 250°C using zinc and tellurium solid source effusion cells, and a microwave plasma source to introduce oxygen or nitrogen. Oxygen or nitrogen flow rates of up to 1 sccm were used, corresponding to a partial pressure of up to 10^{-5} Torr. ZnTe and ZnTeO samples grown by MBE were performed on GaAs (001) substrates, providing a suitable template for zincblende ZnTe with low concentrations of oxygen or nitrogen. The growth rate for samples grown by MBE was approximately 0.4 nm/s, with a sample thickness of 1.5 μm.

The structural, chemical, and optical properties of the ZnTeO thin films were investigated to study the influence of oxygen incorporation into ZnTe. X-ray diffraction θ–2θ scans were used to determine crystal structure and crystalline orientation. X-ray photoelectron spectroscopy (XPS) was used to detect the presence of oxygen, nitrogen, and associated bonding configurations. Optical reflectance spectra were used to determine layer thickness and to approximate optical absorption characteristics. Optical transmission measurements were performed on samples deposited on *c*-plane sapphire substrates to determine optical absorption spectra. Photoluminescence measurements were also used to more carefully identify the band edge and associated spontaneous emission transitions. Photoluminescence measurements were performed with a HeCd laser operating at 325 nm.

RESULTS

X-ray diffraction measurements for ZnTe samples grown by PLD and MBE on GaAs (001) are shown in Fig. 1a and b, respectively. In the absence of oxygen, zincblende ZnTe (001) is observed for both PLD and MBE growth, corresponding to epitaxial growth on GaAs (001). The introduction of nitrogen or oxygen during the PLD process resulted in the degradation of the ZnTe (002) and (004) crystalline reflections and the absence of additional peaks that would correspond to alternative crystalline structures or orientations. All of the samples grown by MBE, including those with oxygen and nitrogen plasma, demonstrated ZnTe (002) and (004) reflections, indicating a clear ZnTe (001) orientation on GaAs (001). The introduction of oxygen resulted in a decrease in the peak intensity and an increase in the linewidth of ZnTe reflections, indicating some degradation in crystalline quality. This degradation in crystalline structure was more pronounced for samples grown with nitrogen. X-ray diffraction θ–2θ scans of ZnTe films grown on c-plane sapphire by PLD and MBE exhibit different crystalline orientation in comparison with growth on GaAs (001). ZnTe deposited by MBE on sapphire (0001) with low oxygen and nitrogen flow exhibited a polycrystalline material with a dominant zincblende (111) orientation. ZnTe deposited by PLD under high oxygen and nitrogen pressure exhibited weak diffraction peaks corresponding to polycrystalline zincblende material, suggesting a low degree of crystallinity and/or amorphous material. There is no evidence of the wurtzite structure of ZnTeO for any of the samples studied.

XPS measurements focusing on tellurium for samples grown by PLD and MBE are shown in Fig. 2a and b, respectively. PLD samples deposited without oxygen or nitrogen show a clear peak corresponding to Te 3d 3/2 and 5/2. PLD deposition under nitrogen ambient shows degradation of these peaks. PLD deposition under oxygen ambient shows clear degradation and disappearance of the Te 3d 3/2 and 5/2 peaks, and appearance of TeO_2 3/2 and 5/2 peaks, indicating the formation of tellurium oxide. XPS measurements of all MBE samples measured indicate the presence of only Te 3d 3/2 and 5/2 peaks, both with and without oxygen incorporation. No TeO_2 3/2 and 5/2 peaks could be identified for XPS scans on MBE samples, suggesting that tellurium oxide compounds are not formed under the MBE growth conditions studied.

For PLD samples, estimated from XPS measurement, the stoichiometry of films grown under

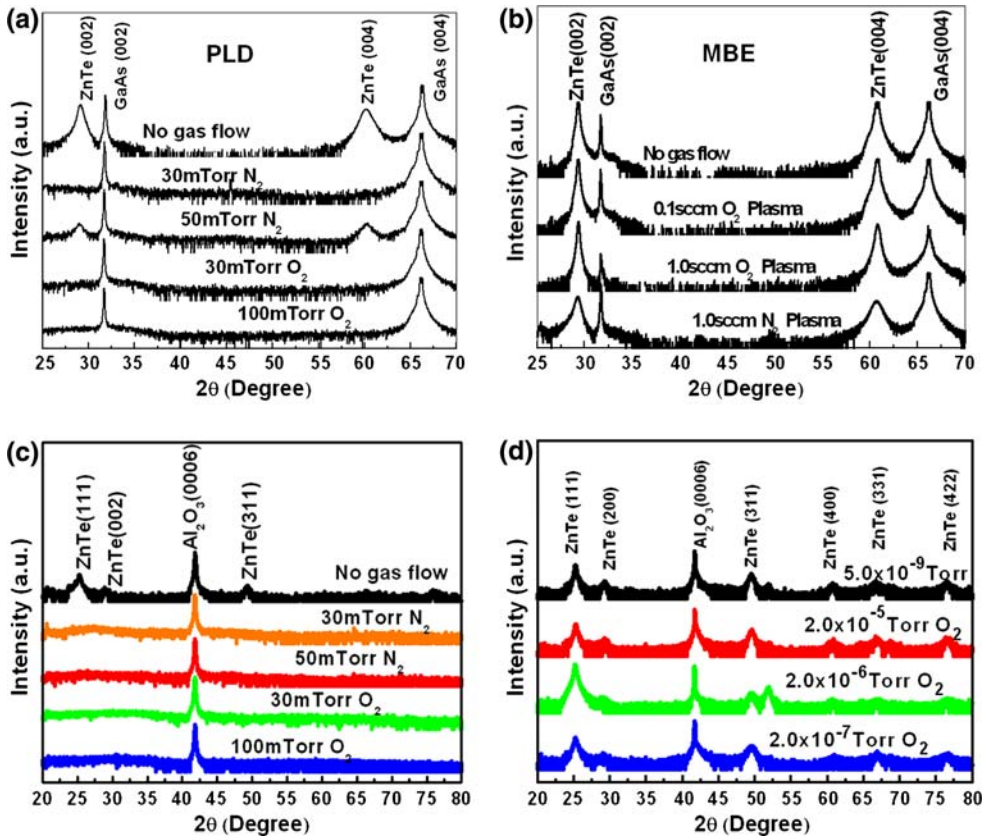

Fig. 1. X-ray diffraction θ–2θ measurements of (a) ZnTe deposition by PLD under varying oxygen and nitrogen partial pressure on GaAs substrate, (b) ZnTe growth by MBE with and without the introduction of oxygen or nitrogen by a plasma source on GaAs substrate, (c) ZnTe deposition by PLD under varying oxygen and nitrogen partial pressure on c-sapphire substrate and (d) ZnTe growth by MBE with and without the introduction of oxygen or nitrogen by a plasma source on c-sapphire substrate.

30 mTorr oxygen was Zn:Te:O = 0.49:0.26:0.25. The stoichiometry of films grown under 100 mTorr oxygen was Zn:Te:O = 0.46 = 0.24:0.31. There is a clear zinc deficiency for samples deposited under high oxygen pressure. For oxygen-doped ZnTe films grown by MBE under all oxygen partial pressure from 2.0×10^{-7} Torr to 2.0×10^{-5} Torr, oxygen concentration was too low to be detected by XPS measurement. Assuming similar incorporation rates for nitrogen and oxygen, the oxygen concentration in ZnTe grown with 2×10^{-5} Torr oxygen partial pressure is estimated to be near 10^{19} cm^{-3}.

ZnTe films deposited under PLD are all highly resistive. ZnTe films deposited by MBE without oxygen or nitrogen are slightly *p*-type with a hole concentration in the mid 10^{14} cm^{-3} range and a mobility of around 20 cm^2/V s. ZnTe films with oxygen doping by MBE are highly resistive. ZnTe with a nitrogen doping by MBE is highly *p*-type conductive with hole concentration and an electron mobility of approximately 1.0×10^{19} cm^{-3} and 40 cm^2/V s, respectively.

The samples grown by PLD under varying oxygen and nitrogen ambient demonstrate dramatic changes in optical transparency, as shown in Fig. 3a. Visual inspection of samples grown on sapphire indicates samples changing from a red color to increasing transparency for increasing oxygen partial pressure, while becoming increasingly opaque for increasing nitrogen pressure. Optical reflectance measurements (Fig. 3b) are consistent with the changing optical transparency, where reduced attenuation of interference fringes is observed at higher energies for increasing oxygen partial pressure. Optical transmission spectra also support these observations (Fig. 3c), where increasing optical transparency is observed at short wavelengths for increasing oxygen partial pressure, and a decrease in transparency for nitrogen incorporation. It should be noted that, whereas an optical transparency change is observed for increasing nitrogen or oxygen pressure, the turn-on characteristic exhibits a more gradual slope. This behavior will be addressed in more detail in the "Discussion" section.

The optical transparency of all MBE samples, on the other hand, demonstrates a shift to lower energy with respect to undoped ZnTe for both oxygen and nitrogen incorporation. The observed shifts in optical reflectance are less dramatic than those observed for PLD samples. The optical reflectance

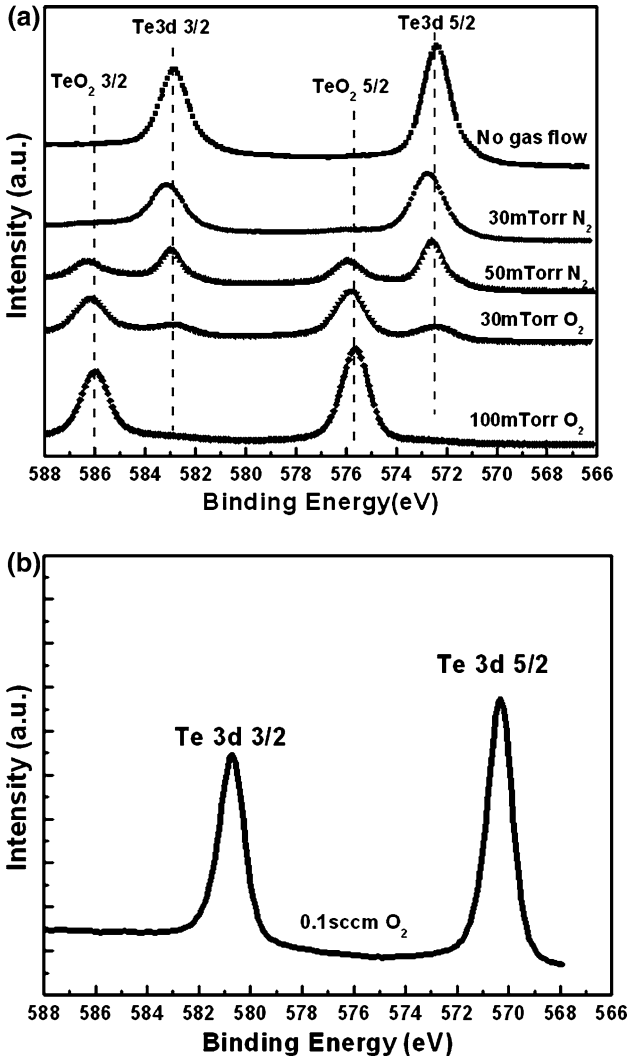

Fig. 2. X-ray photoelectron spectroscopy of (a) ZnTe samples deposited by PLD under varying oxygen and nitrogen partial pressure and (b) a representative ZnTe sample grown by MBE with 0.1 sccm oxygen flow through a plasma source.

spectra for two MBE samples under 0.1 sccm oxygen flow with varying thickness are shown in Fig. 4a, indicating increased optical attenuation below the ZnTe band edge for higher sample thickness. Optical transmission spectra of samples with varying oxygen pressure clearly show increased absorption at energies below the ZnTe bandgap (Fig. 4b). In contrast to the gradual shift in transmission observed for PLD samples, oxygen incorporation in the MBE samples demonstrates a resonant-like behavior near 650 nm (1.9 eV). Transmission curves were used to extract the optical absorption coefficient. The transmission equation for a two-layer (ZnTe or ZnTeO/on sapphire substrate) film can be expressed as

$$T = \frac{(1 - R_1 T_x)\mathrm{e}^{-\alpha d}}{1 - R_1 R_x \mathrm{e}^{-2\alpha d}}, \qquad (1)$$

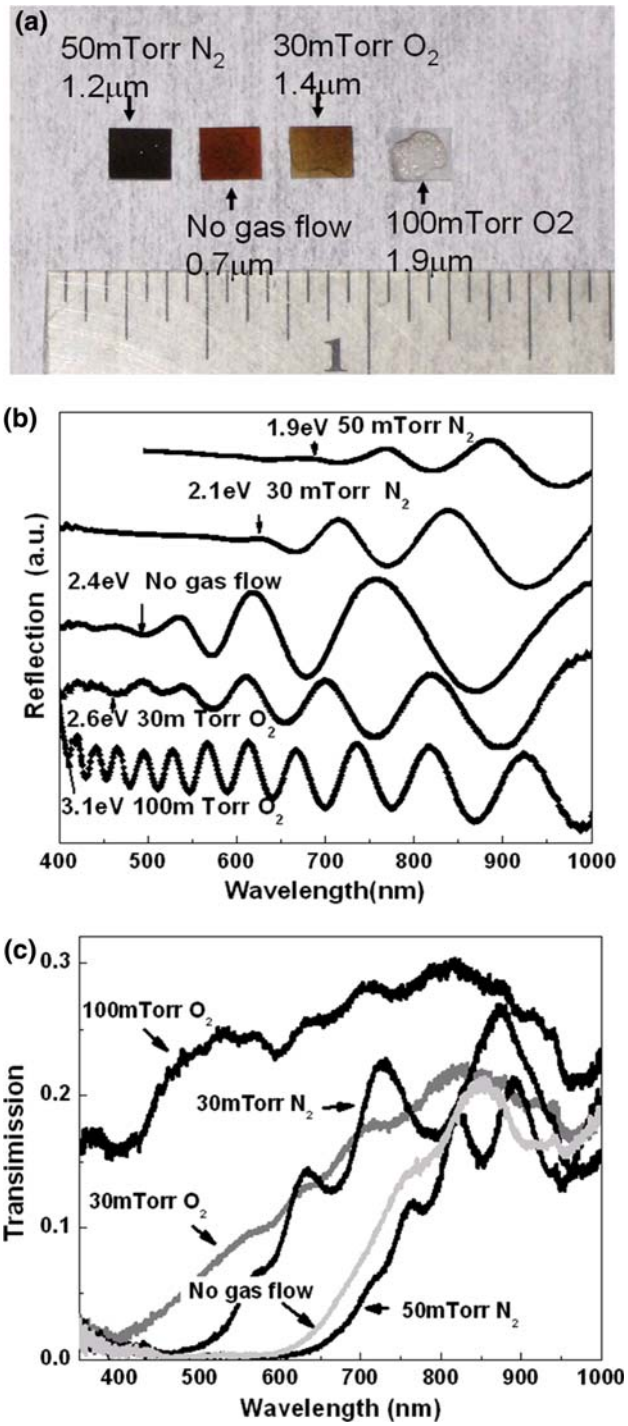

Fig. 3. Optical transparency of ZnTe samples deposited by PLD under varying oxygen and nitrogen partial pressure as shown by (a) photograph, (b) reflectance spectra, and (c) transmission spectra.

where α is the optical absorption coefficient and d is the layer thickness. The transmission and reflection components T_x and R_x are then given by

$$T_x = \frac{(1 - R_2)(1 - R_3)}{1 - R_2 R_3}. \qquad (2)$$

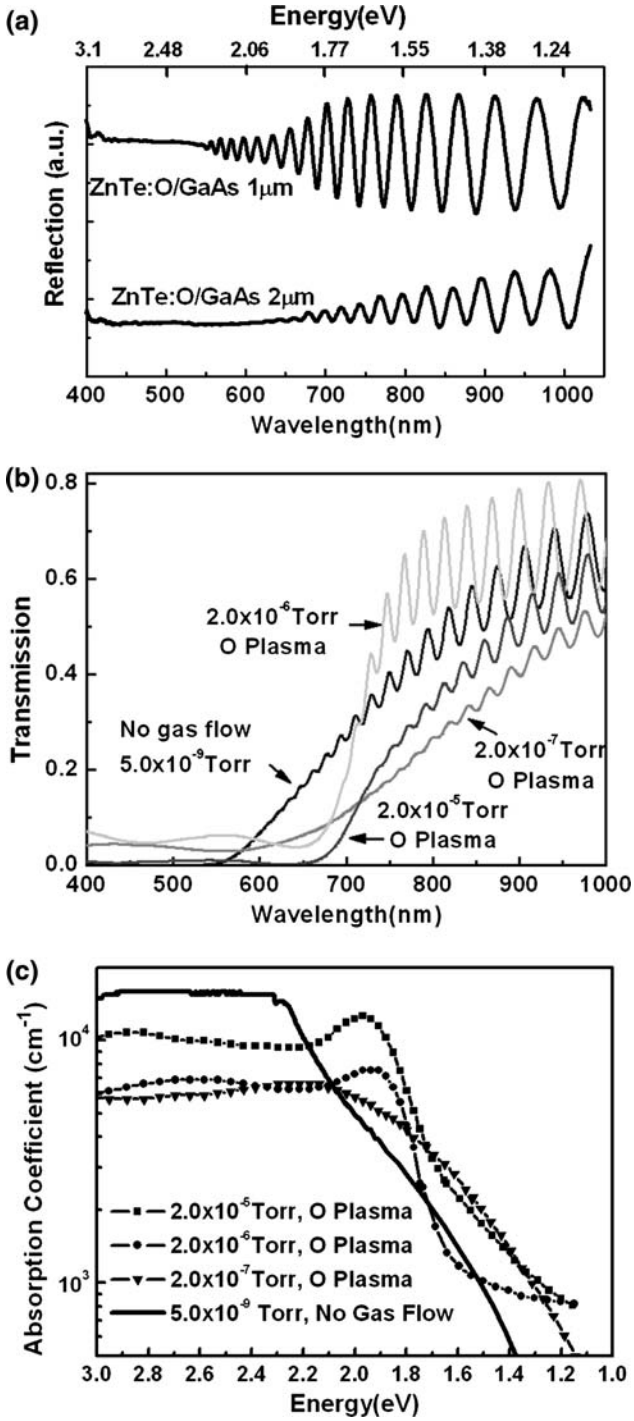

Fig. 4. Optical transparency of ZnTe samples grown by MBE with oxygen plasma as shown by (a) reflectance spectra, (b) transmission spectra, and (c) absorption coefficient spectra extracted from transmission measurements.

$$R_x = R_2 + \frac{R_3(1-R_2)^2}{1-R_2R_3}. \quad (3)$$

In Eqs. 1 and 2, $R_1 = (1-n_1)^2/(1+n_1)^2$, $R_2 = (n_1-n_2)^2/(n_1+n_2)^2$, and $R_3 = (n_2-1)^2/(n_2+1)^2$ are

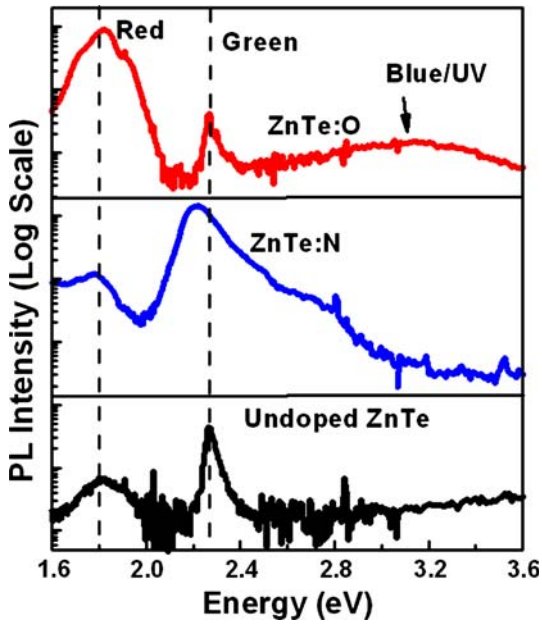

Fig. 5. Room-temperature photoluminescence spectra of undoped, nitrogen-doped, and oxygen-doped ZnTe.

the interface reflections of air/ZnTe(or ZnTeO), ZnTe (or ZnTeO)/sapphire, and sapphire/air, respectively, where n_1 and n_2 are wavelength-dependent refractive indices of ZnTe[14] and sapphire. The index of refraction of ZnTeO was assumed to be the same as ZnTe. The extracted absorption coefficient spectra of ZnTe and ZnTeO are shown in Fig. 4c.

Photoluminescence spectra were measured for MBE samples, as shown in Fig. 5. Samples deposited by PLD only demonstrated very weak PL characteristics, which were degraded further upon oxygen and nitrogen doping, and were therefore not studied in this work. MBE samples grown without nitrogen or oxygen demonstrate a predominant peak near 2.3 eV, corresponding to the ZnTe band edge. Emission at longer wavelength, near 1.8 eV, is also observed and may be attributed to deep-level defects and/or unintentional background oxygen incorporation. For ZnTe with nitrogen incorporation, the band-edge transition becomes broadened and moves to lower energy near 2.2 eV. The altered band-edge emission may be attributed to the incorporation of nitrogen acceptor states. For oxygen doping, a dramatic increase in net PL emission is observed, with a dominant transition near 1.8 eV. In addition to the dominant peak at 1.8 eV, oxygen doped samples exhibit a peak at 2.3 eV corresponding to ZnTe, as well as a peak in the 3.0 eV to 3.4 eV range that may be related to the formation of ZnO or a related ZnOTe alloy.

DISCUSSION

The PLD process, providing conditions of high oxygen or nitrogen partial pressure, provides dramatic changes in optical transparency. These

changes may be attributed to the formation of tellurium oxide (oxygen incorporation), or incorporation of nitrogen acceptors (nitrogen incorporation). The formation of tellurium oxide is apparent based on XPS measurements where TeO_2 bonding is observed, increased optical transparency corresponding to the larger bandgap of this material, and lack of crystal structure observed by x-ray diffraction. The gradual transmission spectra observed for oxygen incorporation, and the presence of some degree of Te 3d bonding in XPS, suggests that these thin films consist of a composite of both ZnTe and amorphous TeO_x. The formation of crystalline semiconducting Zn(Te,O) alloys is clearly inhibited for the PLD process under the conditions studied, possibly requiring the introduction of reactive oxygen in the form of a plasma source or ozone. However, the formation of the amorphous ZnTeO composite may provide a valuable technique for integrated optical/electronic devices based on this material system where optically transparent and/or electrically insulating layers are needed.

The MBE samples studied in this work clearly show that Zn(Te,O) alloys are achievable in the ZnTe zincblende crystal structure. X-ray diffraction measurements indicate slight degradation in the crystal structure, but this degradation is relatively minor in comparison with nitrogen doping. XPS measurements indicate that oxygen incorporation is primarily due to O-Te substitution, rather than the formation of TeO_x. The resonant-like optical absorption below the ZnTe band edge for samples grown with oxygen indicates the presence of an efficient optical transition corresponding to an optically active defect level or ZnTeO alloy with intermediate band or large bandgap bowing. For an oxygen concentration lower than a threshold value,[15] typically near 10^{18} cm^{-3}, the oxygen state is localized. The energy level of the oxygen state is fixed at 0.4 eV below the conduction band edge where the energy level is determined by the difference of electronegativity between atomic oxygen and tellurium.[7,16] With increasing oxygen concentration, oxygen states will be coupled as oxygen–oxygen pairs, or oxygen clusters[17,18] with the energy level shifting further away from the conduction band. With a further increase in oxygen concentration, typically Te/O ratio of 1%, an intermediate band may be formed whose energy level shifts with oxygen concentration.[11] At higher oxygen concentration, a phase separation is believed to occur due to the differing crystal structure for ZnTe and ZnO. Tellurium oxide may also be formed, as demonstrated in our ZnTeO films grown by PLD. The extreme case of ZnTeO is tellurium-doped ZnO, where the valance band of ZnO may be shifted to higher energy.[19] The spectral position of the optical transition near 1.8 eV observed in optical absorption and PL spectra for oxygen-doped samples is consistent with previously reported oxygen defects in ZnTe.[10,11,20,21] Since the maximum oxygen concentration in our sample is about 1×10^{19} cm^{-3}, the optical transition in our samples is believed to result from oxygen pairs or oxygen cluster instead of the formation of an intermediate band alloy where a shift with oxygen concentration would be expected. The large absorption coefficient observed, however, is more consistent with a higher density of states than would be typically observed for a defect level transition. The strong radiative emission and absorption properties of these ZnTeO thin films is useful for optical emission or optical conversion devices, as well as an impurity band or intermediate band detector that is currently sought for high-efficiency solar cells.[22,23]

CONCLUSION

Oxygen incorporation is demonstrated in ZnTe samples synthesized by PLD and MBE. The high oxygen partial pressure in the PLD process was found to result largely in the formation of amorphous TeO_x, where thin film exhibit increasing optical transparency in the visible spectral region. These thin films may find application as electrically insulating or optically transparent layers for electronic or optical devices based on ZnTe, ZnO, or related semiconductor material systems. The low oxygen content and active oxygen component in the MBE process was found to result in the formation of ZnTe with a defect band or intermediate band 0.4 eV below the band edge. The defect or intermediate band resulting from oxygen incorporation exhibits high radiative efficiency and strong optical absorption properties, and may be useful for optical emitters/converters or intermediate/defect band solar cells.

ACKNOWLEDGEMENT

This work is supported by the Center for Optoelectronic Nanostructured Semiconductor Technologies, a DARPA UPR Award HR0011-04-1-0040.

REFERENCES

1. S.O. Ferreira, H. Sitter, W. Faschinger, and G. Brunthaler, *J. Cryst. Growth* 140, 282 (1994). doi:10.1016/0022-0248(94)90300-X.
2. C.M. Rouleau, D.H. Lowndes, J.W. McCamy, J.D. Budai, D.B. Poker, D.B. Geohegan, A.A. Puretzky, and S. Zhu, *Appl. Phys. Lett.* 67, 2545 (1995).
3. J. Han, T.S. Stavrinides, M. Kobayashi, R.L. Gunshor, M.M. Hagerott, and A.V. Nurmikko, *Appl. Phys. Lett.* 62, 840 (1993).
4. I.W. Tao, M. Jurkovic, and W.I. Wang, *Appl. Phys. Lett.* 64, 1848 (1994).
5. J.D. Dow, R.-D. Hong, S. Klemm, S.Y. Ren, M.-H. Tsai, O.F. Sankey, and R.V. Kasowski, *Phys. Rev. B (Condens. Matter)* 43, 5396 (1991).
6. K. Akimoto, H. Okuyam, M. Ikeda, and Y. Mori, *J. Cryst. Growth* 117, 420 (1992).
7. J.J. Hopfield, D.G. Thomas, and R.T. Lynch, *Phys. Rev. Lett.* 17, 312 (1966).
8. R.E. Deitz, D.G. Thomas, and J.J. Hopfield, *Phys. Rev. Lett.* 8, 391 (1962).
9. J.D. Cuthbert, J.J. Hopfield, and D.G. Thomas, USA Patent 3413506 (1966).

10. Z.T. Kang, H. Menkara, B.K. Wagner, C.J. Summers, R. Durst, Y. Diawara, G. Mednikova, and T. Thorson, *J. Electron. Mater.* 35, 1262 (2006).
11. K.M. Yu, W. Walukiewicz, J. Wu, W. Shan, J.W. Beeman, M.A. Scarpulla, O.D. Dubon, and P. Becla, *Phys. Rev. Lett.* 91, 246403 (2003).
12. S. Merita, T. Kramer, B. Mogwitz, B. Franz, A. Polity, and B.K. Meyer, *Phys. Status Solidi C* 4, 960 (2006).
13. Y. Nabetani, T. Okuno, K. Aoki, T. Kato, T. Matsumoto, and T. Hirai, *Phys. Status Solidi A* 203, 2653 (2006).
14. D.T.F. Marple, *J. Appl. Phys.* 35, 539 (1964).
15. J.L. Merz, *J. Appl. Phys.* 42, 2463 (1971).
16. J.L. Merz, *Phys. Rev.* 176, 960 (1968).
17. M. Felici, A. Polimeni, M. Capizzi, Y. Nabetani, T. Okuno, K. Aoki, T. Kato, T. Matsumoto, and T. Hirai, *Appl. Phys. Lett.* 88, 101910 (2006).
18. M.J. Seong, I. Miotkowski, and A.K. Ramdas, *Phys. Rev. B (Condens. Matter)* 58, 7734 (1998).
19. H.L. Porter, C. Jin, J. Narayan, A.L. Cai, J.F. Muth, and O.W. Holland, *Mater. Res. Soc. Sypm. Proc.* 744, M5.5.1 (2003).
20. S. Iida, *J. Phys. Soc. Jpn.* 32, 142 (1972).
21. M. Schneider, H. Tews, and R. Legros, *J. Cryst. Growth* 59, 293 (1982).
22. A.S. Brown and M.A. Green, *J. Appl. Phys.* 94, 6150 (2003).
23. L. Cuadra, A. Marti, and A. Luque, *Thin Solid Films* 451–452, 593 (2004).